Chromatin Higher-Order Structure: Results from Small-Angle X-Ray Scattering and Histone-Octamer Crystallography

J. Kilner[1], J.M. Nicholson[2], L. Chantalat[3], S.J. Lambert[4], H.W Rattle[5] and J.P. Baldwin[4]

1 MAFF, York, U.K.
2 Daresbury Laboratory, Daresbury, Warrington, Cheshire WA4 4AD, U.K.
3 Laboratoire de Crystallographie Macromoleculaire, Institut de Biologie Structurale, 41 Avenue des Martyrs, 38027 Grenoble 1, Cedex, France.
4 Biophysics Group, School of Biomolecular Sciences, John Moores University, Byrom Street, Liverpool L3 3AF, U.K.
5 Biophysics Laboratories, University of Portsmouth, White Swan Road, Portsmouth PO1 2QX, U.K.

Introduction

Chromatin is the highly ordered DNA-protein complex, which serves to package and organise the chromosomal DNA in the cell nucleus. It is able to alter the level of DNA packaging, thus playing crucial roles at different stages of the cell cycle. The nucleosome core is the basic unit of chromosome structure, composed of a species-dependent 168 - 240 base pairs of DNA, 146 of which are wound around an octameric histone-protein core containing two dimers of histone proteins, 2(H2A.H2B), complexed with a tetramer of histones, $(H3.H4)_2$. A fifth histone, the linker histone H1 (also H5 in avian erythrocytes), binds to the DNA outside the complex containing the core. The complex of the nine histones plus 168-240 base pairs of DNA is the nucleosome.

The histones are very highly conserved between relatively unrelated species, even between plants and animals, which highlights their crucial role in the chromosome and suggests that all histones are evolutionarily related.

Nucleosomes are strung together over the whole of the DNA in the cell nucleus and form zig-zags in a long chain. The zig-zagging chain folds into a higher-order structure, which is accepted to be a left-handed coil of about six nucleosomes per 10nm and of diameter ~30nm.

Many studies of higher-order structure have been carried out since electron microscopy suggested the existence of the 30nm coil. Perhaps the most notable have been the use of neutron-small-angle contrast variation to show that the histone H5 is on the inside of the structure [1, 2] and optical-transform studies of electron microscopy images showing a left-handed coiled structure [3]. Fibre-diffraction studies, although useful in establishing a 10nm repeat along the fibre [4] and packing of the coils in the fibre [5], have not produced diffraction to high resolution and models for the arrangement of nucleosomes in the core particle abound. Two models seem to have most credibility; the first being where the nucleosomes form the coil and the DNA goes from one nucleosome to the next *around* the coil [6]. The second model is where the nucleosomes interlace back and forth *across* the coil [7].

There are several recent reviews of this field of work [8], but a most crucial missing piece of information is the location of the linker histone which was thought to be located more or less symmetrically at the diad axis of the nucleosome, protecting the DNA from nuclease attack as it enters and as it leaves after two-turns around the octamer histone core [9]. Neutron-scattering results [10, 11] showed that the linker histone has a lower radius from the centre of the histone octamer than would be suggested by such a model and more recently several studies confirm an asymmetric location of linker histones [12].

Results

Small-Angle X-Ray Scattering

One of the problems in studying the higher-order coil of nucleosomes by small-angle scattering is that fractionation of the chains of forty or more nucleosomes needed for the studies (cleaved as polynucleosomes out of cell nuclei by light micrococcal nuclease digestion) can disturb the linker histones. Therefore a method was developed for gently fractionating chick-erythrocyte polynucleosomes on a Sephacryl 1000 column.

X-ray small-angle scattering spectra for non-aggregating "rods" of molecules in solution are analysed by plotting the graph of $sI(s)$ versus s^2 where s is the scattering-angle-θ-dependent parameter $2.\sin\theta/\lambda$ and λ is the wavelength. $I(s)$ is the intensity of scattering, as a function of θ, measured in these experiments by the detector on beam-line 8.2 at the Daresbury Laboratory Synchrotron Radiation Source. The gradient of the graphs, if the rods are rigid and the scatter curves are concentration independent, is a measure of the

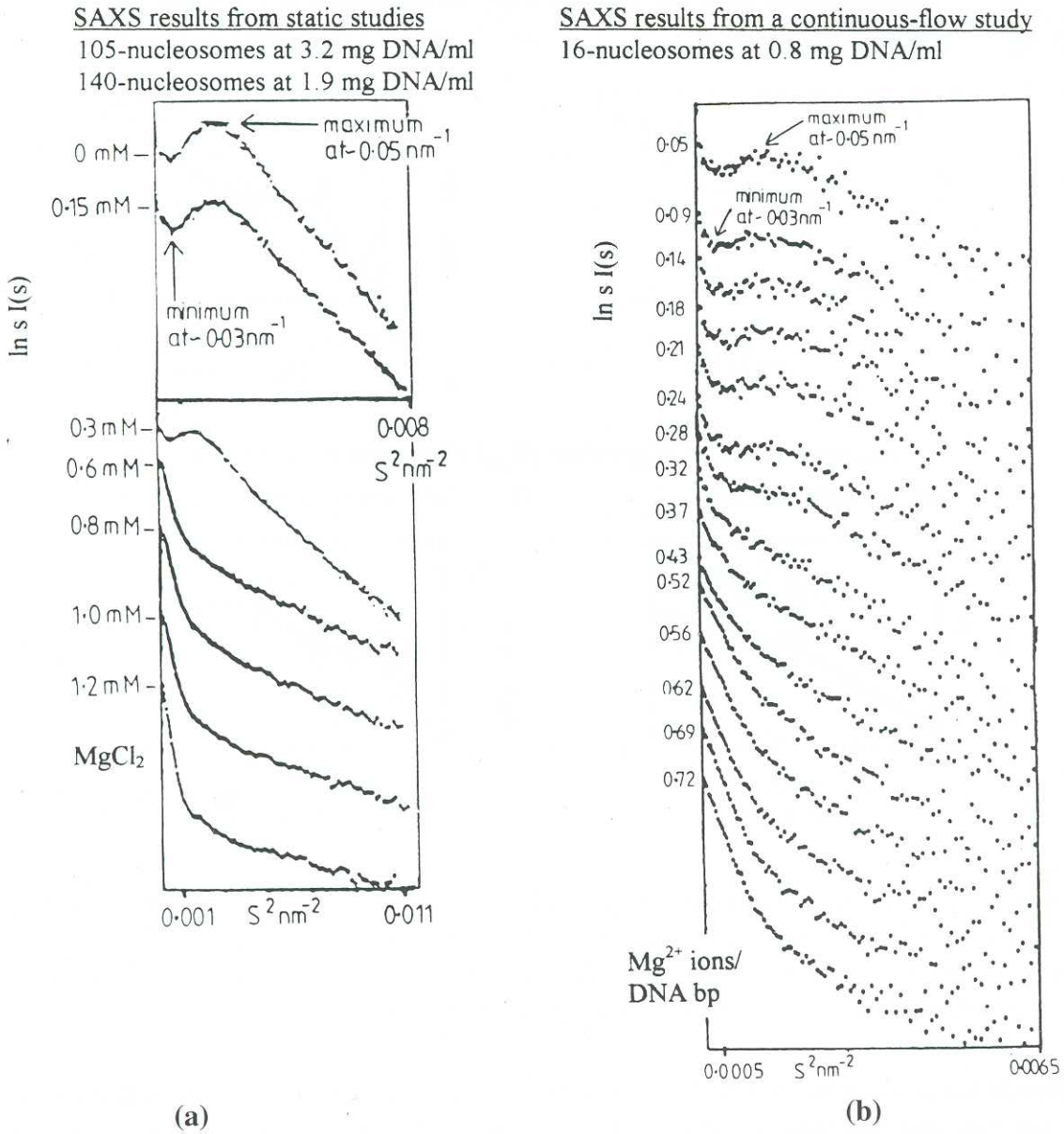

Figure 1: Magnesium-ion dependence of the scattering of X-rays, ln(s.I(s)) vs s^2, where I(s) is the intensity of scattering from solutions of nucleosome multimers. The scattering parameter s is related to the scattering angle 2θ by $s = 4\pi\sin\theta / \lambda$, where λ is the X-ray wavelength. The number of nucleosomes in the multinucleosomes was determined from agarose-gel electrophoresis of the DNA extracted from them, knowing the nucleosome repeat of 210 base pairs in chick erythrocytes. In the static study of Figure 1(a), the magnesium-ion molarity of each solution was known by the dilution used from a stock 1M solution of $MgCl_2$. In the continuous-flow experiment of Figure 1(b), a dialysis cell was used to continuously change and continuously monitor the concentration of magnesium ions. Note that at the end of the folding processes, at low s and the highest magnesium concentrations, the s.I(s) plots from the multinucleosomes showed straight line plots amenable to a rod-Guinier analysis for long chains of multinucleosomes such as in Figure 1(a) (see text) leading to Figures 2 and 3.

square of the cross-sectional radius of gyration. The intercept on the sI(s) axis gives the mass per unit length of the rods if the graphs are put on an absolute scale by calibration from the scattering curve of a standard, in this case scattering from nucleosome core particles. This analysis does not depend on the precise molecular weight of the rods provided the ratio of the length to diameter is greater than about two to three (surprisingly). These criteria were checked in the present experiments and did apply to Figure 1(a). All spectra were checked for any aggregation by photon-correlation spectroscopy studies of the folding pathways.

Figure 1 shows cross-sectional Guinier plots of the multinucleosomes in solution as a function of magnesium-ion concentration as the nucleosomes fold from a zig-zag chain and eventually into the 30nm coil [13]. The magnesium ions were introduced in a continuous way using a dialysis cell specially made for beamline 8.2 and Figure 1(b) shows the folding pathway most clearly, although

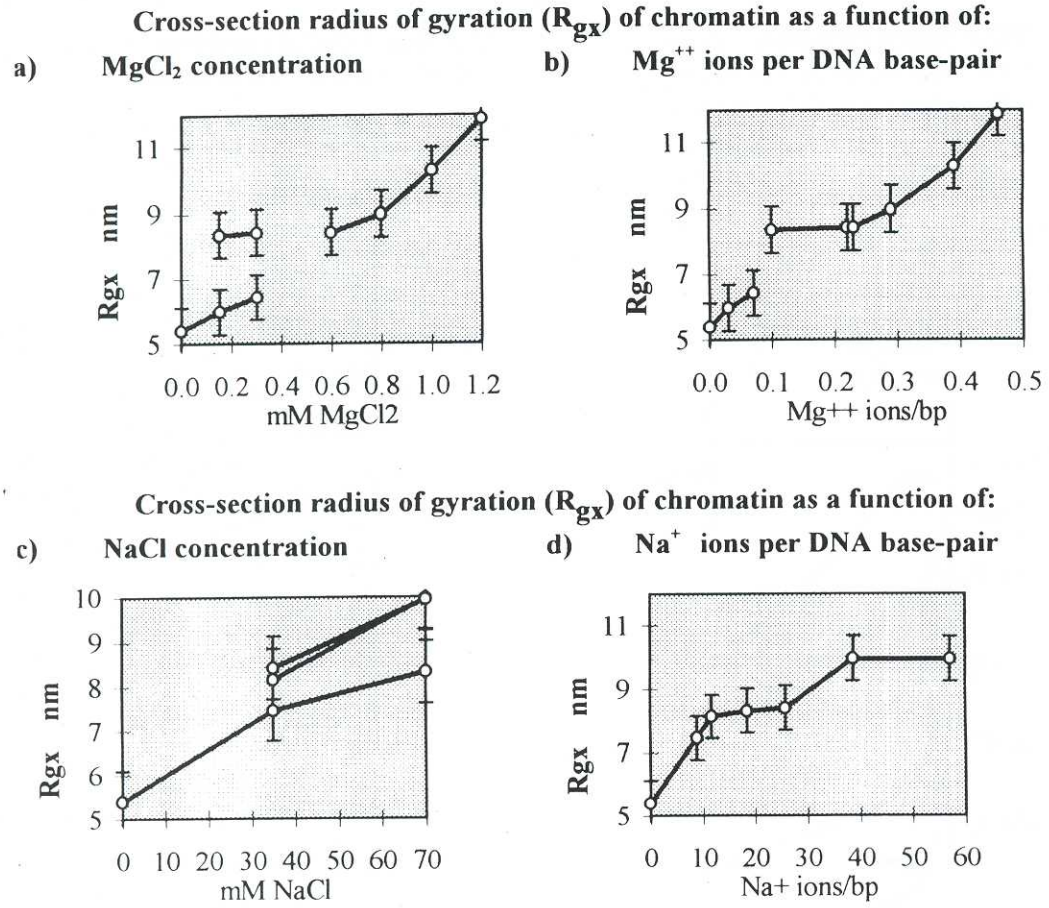

Figure 2: Comparison of the cross-sectional radii of gyration, R_{gx}, of multinucleosomes containing more than 100 nucleosomes, and their dependence on the concentrations of Na^+ and Mg^{2+} ions. The R_{gx} values come from the slopes of the rod-Guinier plots such as Figure 1(a). The curves of the R_{gx} values are more continuous when they are plotted against ions per base pair in the multinucleosomes, calculated from the known molecular weights and DNA concentrations.

these multinucleosomes had too few nucleosomes to carry out the full rod analysis for the scattering curves.

Figure 1(a) shows results for high multimers of nucleosomes where the length to diameter of the rods is high. Straight cross-section Guinier plots are observed near the finally compacted state. Cross-section radii of gyration and mass-per-unit-length values (expressed as numbers of nucleosomes per unit length by calibration of the plots against nucleosome core particles) are plotted against the concentration of Na^+ ions and Mg^{2+} ions in Figures 2 and 3 respectively. Knowing the molecular weight of the nucleosome multimers (from gels of the DNA extracted), the ion concentrations could be calibrated in terms of concentration of ions per base pair for the different measurements with samples at different concentrations of multinucleosomes.

It is clear from Figures 2 and 3 that the compaction of the higher-order coil of nucleosomes depends on the number of ions per base pair.

These studies show in addition that the compaction is greater in Mg^{2+} ions than in Na^+ ions and reaches 6 to 8 nucleosomes per 11nm length of coil with cross-sectional radii of gyration of 10 to 11 nm (coil cross-section diameter about 28 to 31nm). Continuous-flow conductivity measurements and photon-correlation experiments showed that the folding of the polynucleosomes at low ionic strength also was different in Na^+ ions compared with Mg^{2+} ions. Indeed folding in Mg^{2+} did not proceed at all in a fixed volume of sample until the concentration of the ions was typically 0.2 mM.

Histone-Octamer Crystallography

The histone octamer, 2(H2A.H2B).(H3.H4)2, was crystallised in 2M KCl/1.35M phosphate [14] giving a $P6_5$ space group with lattice parameters $a = b =$ 15.8 nm, c = 10.2nm. We solved the structure to 0.215 nm [14,15] resolution, from data collected on beamline 7.2 at Daresbury Laboratory, by molecular replacement using the program AMORE.

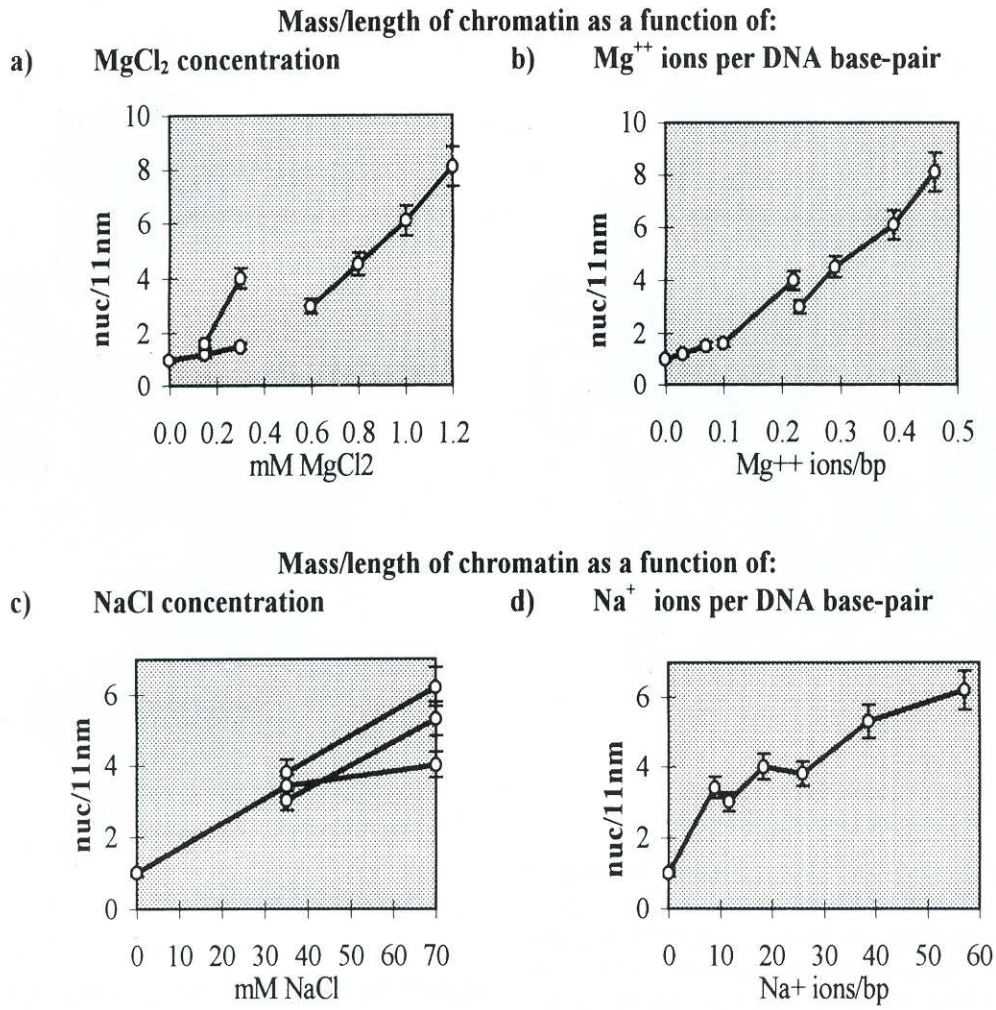

Figure 3: Comparison of the mass per unit lengths of multinucleosomes containing more than 100 nucleosomes and their dependence on the concentrations of Na^+ and Mg^{2+} ions from the same rod-Guinier plots used in Figure 2. These values were calculated from the intercepts of the ln(s.I(s)) vs s^2 plots on the ln(s.I(s)) axis. The data were put on an absolute scale by comparison with the scattering from standard solutions of nucleosome-core particles, so putting the mass per unit lengths in terms of nucleosomes per 11nm length. Note: 11nm comes from the literature on X-ray and neutron diffraction studies of chromatin fibres, where a meridional 11nm equivalent-spacing peak is observed.

Remarkably the crystal consists of left-handed helical arrays of histone octamers with six octamers per 10.2nm-c-axis repeat, which is strikingly similar to what would be the arrangement of histone octamers in the higher-order coil of nucleosomes discussed above. Questions arise therefore about whether the orientation of the octamers in the crystal has any relationship to the orientation of octamers in the coils of multinucleosomes and whether packing interactions between octamers in the crystals relate to interactions in the higher-order structure multinucleosomes in cell nuclei.

It has been suggested by Luger *et al.* [16], from the packing of nucleosome core particles in their $P2_12_12_1$ crystal structure, that the unit-cell packing interactions between basic amino-acid residues 16-25 of histone H4 and an acidic region on the surface of the H2A.H2B dimer may be important in the chromatin higher-order coil structure. This may be the case, of course, but the interactions between the histone-octamer molecules in the octamer crystals are of three types: 1) between residues 14 to 35 of histone H2A of one molecule and residues 24 to 53 of histone H4 of an adjacent octamer; 2) between residues 61 to 91 of histone H2A' of one molecule and residues 53 to 68 of histone H3' of an adjacent octamer; 3) between residues 105 to 120 of histone H2B' of one molecule and residues 21 to 36 of histone H4' of an adjacent octamer. Therefore it is not yet clear that protein-protein interactions between histone octamers directly occur in the higher-order structures of chromatin. The regions where interactions occur are shown on the map of the

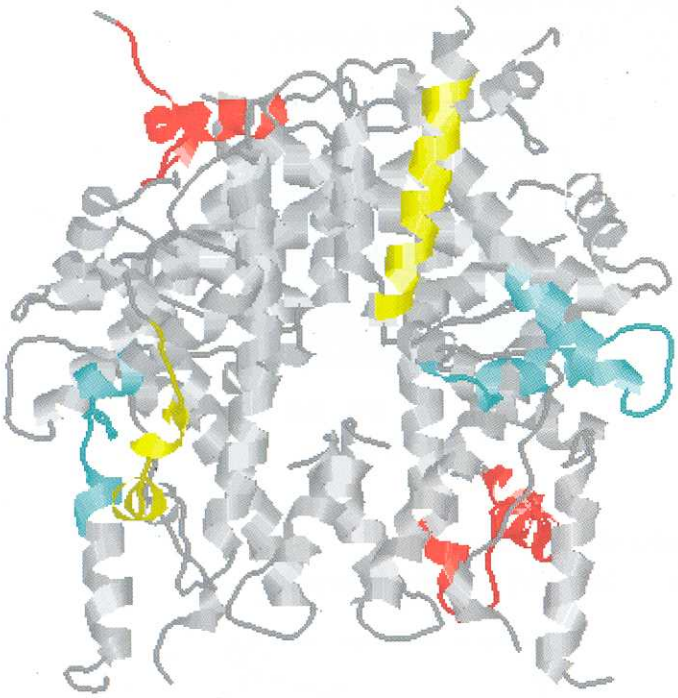

Figure 4: The structure of the histone octamer determined from the single crystal study at 2.15 Å resolution. The regions of interaction between octamers in the crystal structure are shown. Red: residues 14 to 35 of H2A of one molecule interact with residues 24 to 53 of H4 of an adjacent octamer. Blue: residues 61 to 91 of H2A' of one molecule interact with residues 53 to 68 of H3' of an adjacent octamer. Yellow: residues 105 to 120 of histone H2B' of one molecule interact with residues 21 to 36 of histone H4' of an adjacent octamer.

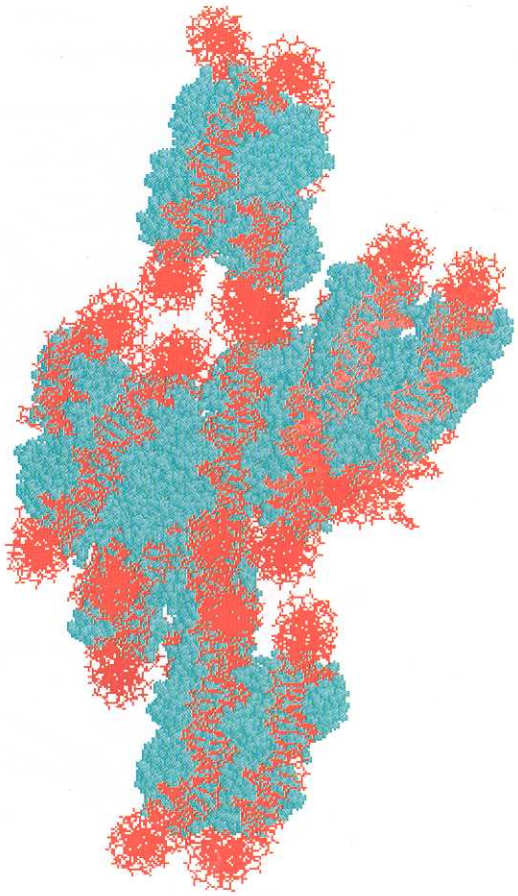

Figure 5: The packed arrays of octamers (blue) in the P65 crystal structure with the DNA (red) from the work of Luger *et al.* grafted on from their PDB file at the correct orientation to the octamers. The DNA fits onto the packed octamers without any clashes.

histone-octamer structure in Figure 4.

The packed arrays of octamers in the $P6_5$ structure are shown in Figure 5, with the DNA from the work of Luger *et al.* grafted on from their PDB file at the correct orientation to the octamers. Remarkably the DNA fits into the structure quite snugly.

Conclusions

Small-angle X-ray scattering studies of multinucleosomes, supported by photon-correlation and conductivity studies, show that Mg^{2+} ions fold the multinucleosomes in a different way from Na^{+} ions to form a more compact rod-like structure, dependent on the number of ions per nucleosome and not on the concentration of ions in the solution. Further the Mg^{2+} ions are "soaked up" by the multinucleosomes at very low ionic strength before the folding of them into a coiled structure commences. Histone octamers in the $P6_5$ crystal structure form helical arrays with parameters remarkably similar to what must be the arrays of octamers in the nucleosomes of chromatin higher structure. Inter-octamer interactions are not the same as in the nucleosome crystal structure, although they may be important in the multinucleosome–coils of chromatin higher-order structure.

Acknowledgements

We are grateful to Professor Colin Reynolds, Dr Fritjof Körber, Dr Amanda Reid, Mr Mike Donovan and Dr Dean Myles for many helpful discussions and support with X-ray facilities at Daresbury Laboratory. We thank Professor Hilary Evans for her encouragement and support from JMU. The work forms part of the Daresbury Laboratory Collaborative Research Program. The EPSRC of the UK gave support with a collaborative research grant.

References

[1] Graziano, V., Gerchman, S.E., Schneider, D.K. and Ramakrishnan, V., *Nature* (1994) **368**, 351-354.

[2] Lasters, I., Wyns, L., Muyldermans, S., Baldwin, J.P., Poland, G.A. and Nave, C., *Eur. J. Biochem.* (1985) **151**, 283-289.

[3] Williams, S.P., Athey, B.D., Muglia, L.J., Schappe, R.S., Gough, A.H. and Langmore J.P., *Biophys. J.* (1986) **49**, 233-248.

[4] Baldwin, J.P., Bosely, P.G., Bradbury, E.M. and Ibel, K., *Nature* (1975) **253**, 245-249.

[5] Widom, J. and Klug, A., *Cell* (1985) **43**, 207-213.

[6] Thoma, F., Koller, T. and Klug A., *J. Cell Biol.* (1979) **83**, 403-427.

[7] Staynov, D.Z., *Int. J. Biol. Macromol.* (1983) **5**, 3-9.

[8] Belikov, S. and Karpov, V., *Febs Lett.* (1998) **441**, 161-164.

[9] Allan, J., Hartman, P.G., Crane-Robinson, C. and Aviles, F.X., *Nature* (1980) **288**, 675-679.

[10] Lambert, S.J., Muyldermans, S., Baldwin, J., Kilner, J., Ibel, K. and Wins, L., *Biochem. Biophys. Res. Commun.* (1991) **179**,810-816.

[11]Baldwin, J.P., *Curr. Opin. Struct. Biol.* (1992) **2**, 78-83.

[12] Hayes, J.J. and Wolffe, A.P., *Proc. Natl. Acad. Sci. USA* (1993) **90**, 6415-6419.

[13] Kilner, J., Ph.D. Thesis (John Moores University 1993).

[14] Lambert, S.J., Nicholson, J.M., Chantalat, L., Reid, A.J., Donovan, M.J. and Baldwin, J.P. , *Acta Cryst. D* (1999) **55**, 1048-1051.

[15] Chantalat, L., Nicholson, J.M., Lambert, S.J., Reid, A.J., Donovan, M.J. and Baldwin, J.P., (submitted).

[16] Luger, K., Mader, A.W., Richmond, R.K., Sargent, D.F. and Richmond, T.J., Nature (1997) **389**, 251-260.

Real Time FTIR and WAXS Studies of the Drawing Behaviour of Polyethylene Terephthalate Fibres

A.C. Middleton[1], R.A. Duckett[1] and I.M. Ward[1], A. Mahendrasingam[2], C. Martin[2]

1 IRC in Polymer Science and Technology, University of Leeds, Leeds LS2 9JT.

2 Department of Physics, University of Keele, Keele ST5 5BG.

The development of molecular orientation and crystallisation has been studied during uniaxial drawing of polyethylene terephthalate (PET) films followed immediately by subsequent taut-annealing at the drawing temperature. The behaviour was monitored in real time throughout both drawing and annealing using dynamic FTIR spectroscopy and in situ WAXS measurements using the Daresbury Synchrotron Radiation Source.

The IR spectra were analysed using curve reconstruction procedures developed previously, and showed that orientation of the phenylene groups and the trans glycol conformers occurred before significant gauche-trans conformational changes could be seen. The onset of crystallisation, defined as the point that the crystalline $\bar{1}05$ reflection could be first observed using WAXS, was not found to correlate with any specific change in the proportions of trans and gauche isomers nor with any feature on the stress-strain curve. However, it was clear that for these comparatively low strain rates, crystallisation occurred during the drawing process, whilst the cross-head was moving, and the draw ratio was increasing.

Introduction

There is considerable evidence from studies of the solid phase deformation of polyethylene terephthalate and related polyesters to show that some aspects can be very well represented by the deformation of a molecular network. In particular, it appears that a molecular network is formed in melt spinning of fibres as the spun yarn cools in the threadline. Provided that no crystallisation occurs, the oriented spun yarn behaves like a frozen stretched rubber, so that a network draw ratio can be defined and quantitative stress-optical measurements can determine the molecular parameters of the network, such as the density of molecular